

The effect of glycyrrhizin acid on *Bax* and *Bcl2* expression in hepatotoxicity induced by Titanium dioxide nanoparticles in rats

Mahmoud Orazizadeh¹, Layasadat Khorsandi¹, Esrafil Mansouri¹, Fereshtesadat Fakhredini^{1,2}

¹Cell & Molecular Research Center, Faculty of Medicine, Ahvaz Jundishapur University of Medical Sciences, Ahvaz, Iran

²Department of Anatomical Sciences, Faculty of Medicine, Ahvaz Jundishapur University of Medical Sciences, Ahvaz, Iran

ABSTRACT

Aim: This research studied the effects of glycyrrhizic acid (GA) on apoptosis induced with by titanium dioxide (NTiO₂) in the liver of rats.

Background: It is widely accepted that the contamination resulting from nanoparticles (NPs) is an emerging dangerous issue. Metal oxide nanoparticles have high environmental stability and cause toxicity in the food chain. Thus, the present study investigated the anti-apoptotic effects of glycyrrhizic acid (GA) on the hepatotoxicity generated by titanium dioxide (NTiO₂) NPs in the liver tissue.

Methods: Thirty-two male Wistar rats were randomly divided into four groups. NTiO₂-treated rats were given 300 mg / kg of NTiO₂ solution via gavage for 14 days; GA-treated were administered 100 mg/kg GA for 14 days; protection group was pre-treated with GA before NTiO₂ administration for 7 days. Then, apoptotic index was evaluated through immunolocalization of Bax and Bcl-2 and TUNEL assay.

Results: we found that HSCORE of Bax expression and apoptotic index experienced a significant increase with NTiO₂ (P <0.001), while Bcl-2 expression significantly diminished in NTiO₂-treated rats (P <0.001). The results revealed that the increased Bax expression and apoptotic index were reversed by GA and enhanced the activities of Bcl2.

Conclusion: The results revealed that GA effectively attenuated apoptosis against NTiO₂ in rats.

Keywords: NTiO₂, Immunohistochemistry, TUNEL, Apoptosis, Histopathological.

(Please cite as: **Orazizadeh M, Khorsandi LS, Mansouri E, Fakhredini FS. The effect of glycyrrhizin acid on *Bax* and *Bcl2* expression in hepatotoxicity induced by Titanium dioxide nanoparticles in rats. Gastroenterol Hepatol Bed Bench 2020;13(2):168-176).**

Introduction

Researchers agree that the liver is a target organ for adverse impacts of xenobiotics. The metabolic functions and strategic location of the liver in close proximity to the gastrointestinal tract and bloodstream have made it highly susceptible to chemical damage, including the detrimental effects of various drugs and chemical pollutants. It is also targeted for various toxins and susceptible to diseases such as liver toxicity (1). Some researchers have found that administrating NPs to the

rodents causes accumulation of NPs in diverse tissues such as the brain, liver, and spleen (2, 3).

Amongst the numerous metal nano-materials, it has been demonstrated that NTiO₂ is utilized in a wide range of consumers' products such as electronics, sunscreen, paints, cosmetics, clothing, and surface coating (4, 5). Further, NTiO₂ is extensively utilized in synthesizing toothpaste, food colorants, and nutritional supplements. The main pathways of exposure to NTiO₂, causing toxic communication, are inhalation and skin exposure. Although most exposure to NTiO₂ is through epidermal contact, numerous studies have reported that NTiO₂ does not cause skin infections (6, 7). Since the respiratory tract is one of the key exposure ways, most investigations on the NTiO₂ have emphasized pulmonary toxicity. For example, Oberdorseter et al. (2002) showed that the NPs were translocated and

Received: 15 September 2019 Accepted: 18 December 2019

Reprint or Correspondence: ereshtesadat fakhredini, PhD. Department of Anatomical Sciences, Faculty of Medicine, Ahvaz Jundishapur University of Medical Sciences, Ahvaz, Iran

E-mail: ffakhredini_aot@yahoo.com

ORCID ID: 0000-0002-7766-3369

accumulated in the liver after the inhalation of carbon particles (8). In addition, Fabian et al. (2008) examined Tissue distribution and toxicity of intravenously administered titanium dioxide nanoparticles in rats. Male Wistar rats were treated with single intravenous injections of a suspension of TiO₂ in the serum (5 mg/kg body weight), and the tissue content of TiO₂ was determined 1, 14, and 28 days later. TiO₂ levels were retained in the liver for 28 days (9). Sugibayashiet et al. (2008) achieved the same outcomes (10).

It has been shown that NTiO₂ has apoptotic effects on several cell lines such as brain cells (11), osteoblasts (12), and induction of necrosis in fibroblasts (13). TiO₂ NPs can penetrate hepatocytes of liver, which is an active organ for detoxification. Liu et al. (2009) (14) observed a considerable reduction of the body weight of the rat treated with nano anatase TiO₂ and an increase in the weight of the liver. Ma et al. (2009) (15) found that TiO₂ NPs damage the liver function and induce an oxidative stress attack causing hepatotoxicity. Li et al. (2012) (16) reported the levels of gene expression through TiO₂ NPs associated with reactive oxygen species (ROS) and cytochrome p450 (CYP1A). In addition, CYP1A activation causes creation of free radicals and ROS, which initiate lipid peroxidation and protein oxidation and cause damages to the hepatocellular membranes. This is followed by releasing inflammatory mediators from the activated hepatic macrophages that cause hepatic necrosis.

Herbal medicines produced from herb extracts have been applied for treating a wide range of clinical illnesses. Note that the defensive impacts of natural anti-oxidants against chemical-induced toxicity have been studied extensively (17,18). Liquorice has been used in food and as medicine for several centuries. Further, licorice root, which is called 'sweet root', consists of compounds almost 50 times sweeter compared to sugar (18).

A study found that glycyrrhizin acid (GA) is one of the natural constituents of liquorice separated from the dried root of *Glycyrrhizaglabra*. It has also been observed that GA salts have extensive applications as aromatizes and sweeteners in sweets, drugs, beverages, chewing-gum, chewing tobacco, and toothpaste (19). Meanwhile, some researchers have demonstrated several pharmacologic impacts of GA such as anti-inflammatory, neuro-protection, antiviral, antitumor, antioxidant (20–26) as well as hepatoprotective activity (26–31). Since the

number of patients with liver failure has increased in recent years and liver disorders are the leading to mortality in today's world, we therefore evaluated the therapeutic effect of GA on NTiO₂-induced apoptosis in hepatocytes and examined the structure of the liver tissue (32-35).

Methods

Animals

The study participants consisted of 32 adult male Wistar rats (age: ranging between 8 and 10 weeks with a weight of 180 to 220 g). Ahvaz Jundishapur University of Medical Sciences, Experimental Research Center was selected to prepare the animals. The ethics committee (CMRC-81) of Jundishapur University gave the approval of the current research. According to the research design, the rats were kept under standard laboratory conditions (a 12 h dark & 12 h light cycle, relative moisture of 50±5% & temperature of 22 ± 3 °C) for a minimum of one week prior to testing. The above conditions were conserved until the test was ended.

Experimental design

Based on the research protocol, the animals were classified into four groups of eight animals randomly:

Group 1: Control group, received saline by gavage for 21 days.

Group 2: GA group, received 100 mg/kg glycyrrhizic acid (GA) by gavage for 21 days.

Group 3: NTiO₂-intoxicated group, 0.2 ml saline was administered for 7 days, and then 300 mg/kg NTiO₂ was given for 14 days.

Group 4: Protection group, 100 mg/kg GA was administered for 7 days, and then GA (100 mg/kg) plus NTiO₂ (300 mg/kg) was given for 14 days.

According to the research design, the dosages of NTiO₂ (Sigma) were chosen based on earlier investigations revealing considerable poisonousness in animals (36). When the NTiO₂ NPs were characterized (outcomes not presented), we procured the stock solution (2 mg/ml) in distilled water. Then, we distributed it for ten minutes by a sonicator. Afterwards, the stock solution of NTiO₂ was placed at temperature of 4 °C and utilized over 1 week. Just before the experiment, the stock solution was diluted using distillate water and dispersed through ultrasonication (Solid State/Ultrasonic FS-14: Fisher Scientific) for fifteen minutes in order to

170 The effect of glycyrrhizin acid on Bax and Bcl2 expression

avoid accumulation. In order to ensure the non-accumulation of NTiO₂ prior to administration, oral gavage was performed over <20 minutes after preparation. Next, after 20 min past the procurement, the size of the NTiO₂ particle was measured using atomic force microscopy (AFM). We dissolved 4200 mg of GA (sigma) in 90 cc of saline. The GA dosage was chosen according to the outcomes of earlier research (37) and our pilot study. In brief, diverse dosages of GA (10, 50, 100, 200 mg/kg) were studied for 2 weeks prior to the test to obtain the most acceptable dosage for protecting the liver with four rates utilized to study all dosages. Biochemical tests including ALT and AST were evaluated after 14 days. ALT and AST were significantly reduced at the doses of 200 and 100 mg/kg (Fig. 2). Thus, we used GA at the dose of 100 mg/kg in this experiment. Then, 1 day following the final administration, animals were killed via anesthesia and their livers were removed. Afterwards, formalin 10% was used to fix them for immunohistochemistry analysis.

Biochemical tests

The blood sample were collected in a heparinized centrifuge tube and centrifuged. The plasma enzyme levels including plasma alanine aminotransferase (ALT) and aspartate aminotransferase (AST) were determined spectrophotometrically from plasma samples using commercially available kits (Sigma).

Immunohistochemistry assay

The current research carried out deparaffinization and rehydration for Bax and Bcl-2 immunoreactivity using xylene and alcohol. Then, distilled water was used to wash them, and citrate buffer (10 mmol/L) was employed for pretreatment of the sections into a microwave oven for 20 min. Then, 1% H₂O₂ for 20 min and a protein block solution (Dako, Carpinteria, CA) were used to treat these sections for 10 min. In order to specify the expression of Bcl-2 and Bax proteins, the rat monoclonal antibody against Bcl2 (sc-7382, Santa Cruz) and Bax (sc-20067, Santa Cruz) in 1:50 was utilized for 90 minutes. Accordingly, 1:300 peroxidase-conjugated streptavidin (Dako A/S) and 1:200 bio-tinylated anti-rat antibodies (Dako A/S; Copenhagen: Denmark) were used to incubate the sections. Lastly, 3, 3'-diaminobenzidine (DAB) tetra-hydrochloride (Sigma; St Louis: MO) was utilized for establishing the peroxidase reaction and hematoxylin for counterstaining. Immunostaining intensity was assessed by a

semiquantitative score called HSCORE technique. This method was computed for all sections via applying the subsequent algorithm (38); that is, $HSCORE = \sum P_i (i+1)$ where *i* refers to the staining intensities (0: no staining, 1= weak, 2= moderate, 3=strong). *P_i* refers to the percentages relating to the stained cells of each individual intensity (0 to 100%).

TUNEL assay

In-Situ Cell Death Detection Kit, POD (Boehringer Mannheim GmbH; Mannheim; Germany) was utilized to detect the particles at a single cell level according to the labeling directions of the DNA strand breaks. Then, the paraffin sections were dewaxed. Afterwards, rehydration of the sections was performed using common techniques. Next, protease was added and incubation was performed with 5% of suitable normal serum (for 30 minutes at 37 °C). Then, phosphate buffered saline was used to rinse the slides. After permeation of sections for two minutes on ice, TUNEL reaction mix was used to incubate them for 60 minutes at 37 °C. After adding Antifluorescein-AP, they were incubated for 30 min again at 37 °C. Accordingly, PBS was used to wash the sections, and incubation was done for 20 minutes using the substrate. Then, light microscopy was employed to analyze them. Afterwards, apoptotic index (AI) was computed via dividing the number of TUNEL-positive germ cell in a randomly focused somniferous tubule by the total numbers of the germ cells in that tubule. Next, the obtained outcome was multiplied by 100. Finally, AIs corresponding to the ten randomly chosen tubules for all spermatogenic steps were assessed, and thus the average AI of all cases was computed (39).

Statistical analyses

According to the research design, one-way ANOVA and post-hoc LSD test were used to analyze the data. The results are expressed as the mean±SD. In addition, *p* greater than 0.05 was regarded statistically significant.

Results

Nanoparticle characterization

As seen, AFM showed the dimension and morphology of the prepared particles. It was indicated that complexes had spherical shapes with an average dimension less than 100 nm (Figure 1).

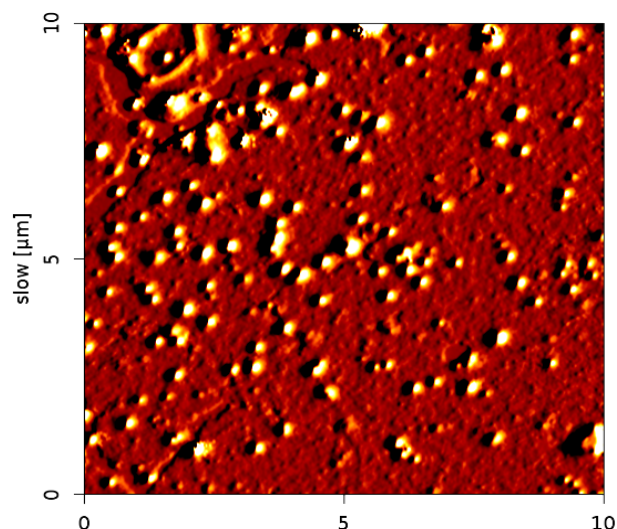


Figure 1. AFM image of NTiO₂ showed distinct spherical particles in the size range between 50 and 100 nm.

Biochemical tests

ALT and AST were evaluated after 14 days. ALT and AST were significantly reduced at the doses of 200 and 100 mg/kg (Fig. 2). Thus, we used GA at the dose of 100 mg/kg in this experiment (Figure 2).

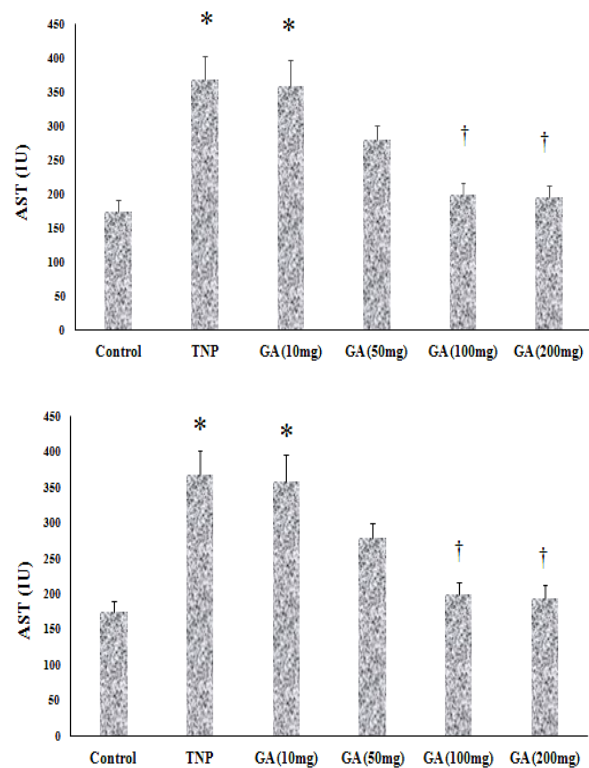


Figure 2. Pilot results for an appropriate dose of GA. The values are expressed as mean \pm SD. (* $P < 0.05$), ($\dagger p < 0.05$). * and \dagger symbols indicate comparison to control and NTiO₂-intoxicated groups respectively.

IHC assessments

A weak IHC reaction was observed in some of the lobules of the control group (Figure 3). The expression pattern of Bax in GA-exposed liver was similar to that of the control group. Also, the results of HSCORE showed no significant difference between them. Further, in most lobules of the NTiO₂ group, Bax was expressed in hepatocytes, especially around the central vein with different color intensities. In addition, HSCORE experienced a significant rise in comparison with the controls and GA groups ($P < 0.001$). Finally, the color intensity and the number of the stained cells in the GA + NTiO₂ group were lower than those of the

NTiO₂ group. Meanwhile, the results of HSCORE showed that Bax expression was significantly reduced in this group in comparison with the rats in NTiO₂ group ($P < 0.001$) (Figure 4).

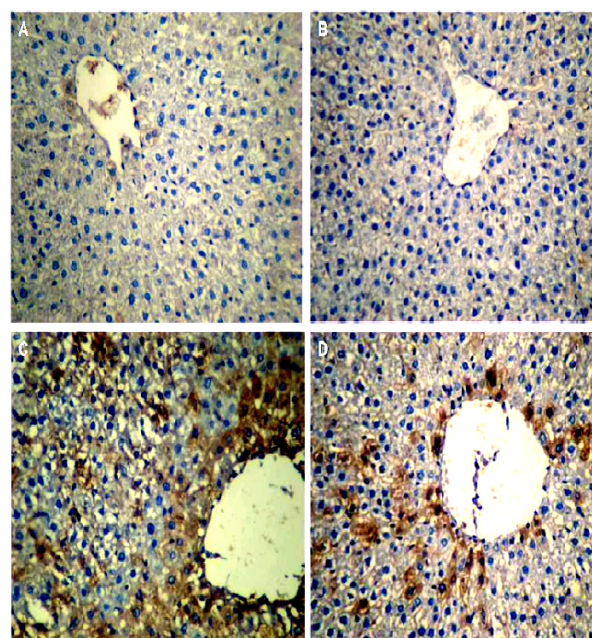


Figure 3. The optical microscope image of the rat liver in the control group (A), GA (B), NTiO₂(C) and GA + NTiO₂ (D) group by IHC staining of Bax protein. In the control group and GA, no color is observed, but in the NTiO₂ group in the cytoplasm, hepatocytes have expressed the Bax (brown) protein. In the GA + NTiO₂ group, this protein is also less pronounced than in the NTiO₂ group (250 \times).

According to the results, in the control group (Fig. 5), Bcl-2 was expressed around the central vein. In the GA group (Figure 5), the expression pattern of Bcl-2 was similar to that of the control group and the results of HSCORE showed no significant difference between

them (Figure 6). However, in the NTiO2 group (Figure 5), the number of the stained cells and color intensity were lower than those of the control and GA groups. In addition, the results of HSCORE showed a significant fall compared to the GA and control groups (Figure 6). In the GA + NTiO2 group (Figure 5), the color intensity and the number of the stained cells considerably increased compared to the NTiO2 group, and the results of HSCORE also showed a significant growth (Figure 6).

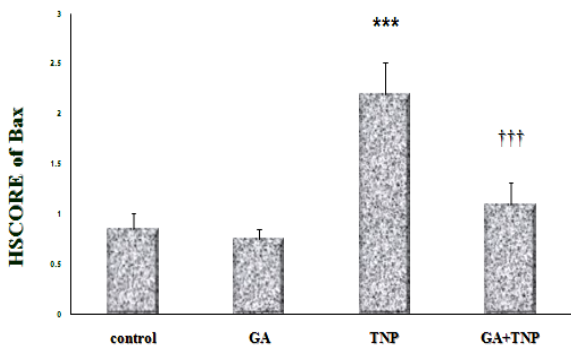


Figure 4. HSCORE assessments of Bax protein in the control groups, GA, NTiO2 and treatment (GA + NTiO2). The values are expressed as mean ± SD. (***) $P < 0.001$, (†††) $p < 0.001$. * And † symbols indicate comparison to control and NTiO2-intoxicated groups respectively.

TUNEL assessments

Spontaneous apoptosis was mostly found in several normal liver hepatocytes associated with the controls (Fig. 7). Based on the results, apoptotic index in the GA group was partially lower compared to the controls ($p > 0.05$). Further, apoptosis was significantly enhanced in all lobules of the NTiO2 group compared to the controls ($p < 0.001$). On the other hand, the apoptotic index in the NTiO2+GA group considerably diminished in comparison with the rats treated with NTiO2 ($p < 0.05$) (Figure 7 and 8).

Discussion

A previous report showed that high concentrations of iron oxide nanoparticles ($150 \mu\text{g} / \text{kg}$) significantly increased the serum levels of the liver enzymes (40). Also, this study demonstrated that GA effectively attenuated apoptosis and histological changes in the hepatotoxicity induced via NTiO2. IHC evaluations revealed that the expression of Bax increased in the hepatocytes of the rats receiving NTiO2 significantly; however, the expression of Bcl-2 in this group significantly decreased.

In addition, some previous studies found that NTiO2 in the liver led to induction of expression of

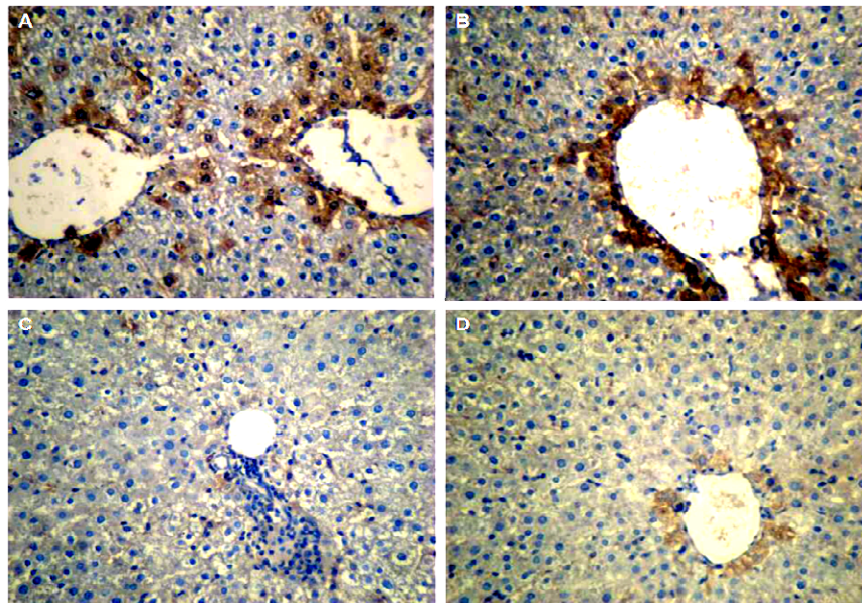


Figure 5. The optical microscope image of the rat liver in the control group (A), GA (B), NTiO2 (C) and GA + NTiO2 (D) group by immunohistochemical staining of Bcl-2 protein. In the control group and GA, the expression of Bcl-2 protein (brown color) is observed, but in the NTiO2 group, the expression of Bcl-2 protein is not observed in hepatocyte cytoplasm. In the GA + NTiO2 group, this protein is more pronounced than in the NTiO2 group (250 ×).

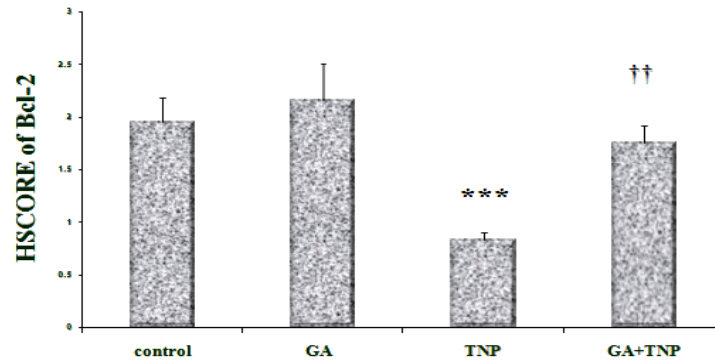


Figure 6. Comparison of Bcl-2 protein expression in control groups, GA, NTiO₂ and treatment (GA + NTiO₂). The values are expressed as mean ± SD (†† p < 0.01), (***) p < 0.001). * and † symbols indicate comparison to control and NTiO₂-intoxicated groups respectively.

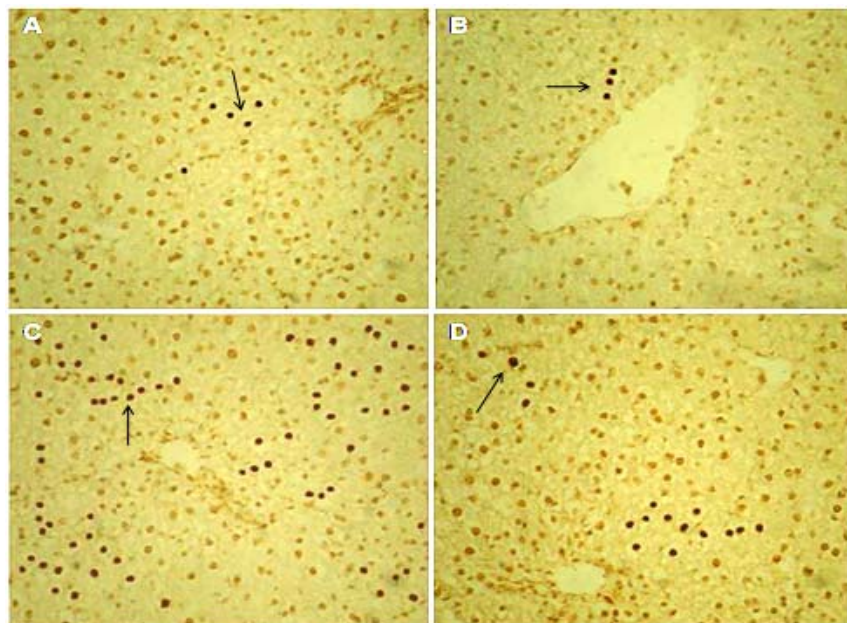


Figure 7. Light microscopy of cross-sections of TUNEL stained liver from control and experimental groups. (A) Control group; (B) GA group; (C) NTiO₂-intoxicated group; (D) NTiO₂ + GA group. Arrows indicate TUNEL-positive reaction. Magnification: 250×

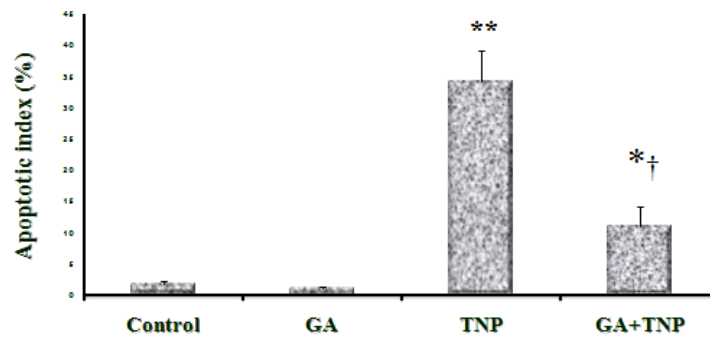


Figure 8. Apoptotic index of control and experimental groups. Values expressed as mean ± SD for 8 mice. **p < 0.01, ***p < 0.001, †† p < 0.01, ††† p < 0.001; * and † symbols respectively indicate comparison to control and NTiO₂-intoxicated group

174 The effect of glycyrrhizin acid on Bax and Bcl2 expression

expression caspase 3, 9 and reduced regulatory expression of Bcl-2 proteins and genes (41). Also, in our study, immunohistochemical analysis of Bax and Bcl-2 protein indicated that the expression of Bax protein in the liver of rats receiving NTiO₂ was significantly enhanced while the expression of Bcl-2 protein in this group was significantly reduced.

Shukla et al. (2011) reported that NTiO₂ induced apoptosis in human HepG2 cell lines in vitro. They reported that administration of very small amounts of NTiO₂ (1 µg / ml) resulted in DNA damage and an increase in the expression of apoptosis proteins such as Cyto-c, Bax, P53, Apaf-1, caspase-9, and caspase-3, as well as the reduction of expression of apoptosis-inhibiting proteins such as Bcl-2 (42). Further, Li et al. indicated that NTiO₂ anatase at 150 mg / kg led to DNA fragmentation of the rat liver cells and eventually apoptosis in these cells (43).

In addition to apoptosis, necrosis was found in the liver tissue of animals treated with NTiO₂ (44). It was demonstrated that apoptosis and necrosis take place in the cells treated with NTiO₂, and the occurrence of a specific cell mortality pattern would be affected by the particles features and the types of cells (45). Further, extensive research has shown that necrosis and apoptosis would not be a fully independent procedure (46), particularly during the apoptosis of several cells (47). According to the IHC and TUNEL outcomes, GA could efficiently reduce the apoptosis and necrosis induced with NTiO₂ in the liver. In addition, the hepatocyte apoptotic index was considerably reduced in the NTiO₂+GA group in comparison with the NTiO₂-intoxicated animals. Another study conducted by Gwak et al. found that GA would attenuate the HMGB1-induced hepatocyte apoptosis (48).

Based on our outcomes, it was found that GA pretreatment suppressed the Bax protein expression though greater Bcl-2 expression. Tang et al. found that GA mitigated endotoxin-induced liver damage after a relative hepatectomy in the rats, and indicated that it considerably reduced the Caspase 3 expression and release of cytochrome c from mitochondrial to cytoplasm. Further, GA enhanced the expression of nuclear genes related with cell proliferation, suggesting the role of this material in hepatic repair (49). Research results in 2007 suggested that gold nanoparticles in the 2–40 nm interval were taken up primarily by Kupffer

cells in the liver and secondarily by macrophages in the spleen and in other places. They stated that endocytosis by macrophages seems not to be the only way that the organism applies to eliminate 2-nanometer gold particles. They hypothesized that part of these tiny nanoparticles was released into the urine as a result of simple in the renal glomeruli (50). Moller et al. found that ultrafine particles cause cytoskeletal toxicity in vitro in macrophages, which can cause cellular dysfunctions, such as impaired proliferation, impaired phagocytic activity, and retarded intracellular transport processes as well as increased cell stiffness, which eventually can result in impaired defense ability in the lungs (51,52). According to our study, it is possible that GA enhances the clearance rate of NTiO₂ in the liver via enhancing the phagocytic capability of the Kupffer cells.

Another study by Duan et al. reported that NTiO₂ led to apoptosis of the spleen cells and that NTiO₂ activated Caspase 3,9, decreased the expression of Bcl-2 proteins and genes, and enhanced the genes expression and proteins of cytochrome C and Bax (53). Studies have also shown that antioxidants such as Green Tea, GSPE, and Resveratrol inhibit apoptosis by controlling the effects of caspases or Bax / Bcl-2 (54).

In conclusion, according to histopathological findings, the present data suggest that GA can effectively protect against NTiO₂- induced apoptosis. Nevertheless, these data should not be readily extrapolated to the human population. However, this information does provide a stimulus for true clinical investigations.

Acknowledgment

This paper was adapted from thesis of Fereshtesadat Fakhredini and was supported by a Grant (CMRC-81) from the research council of the Ahvaz Jundishapur University of Medical Sciences.

Conflict of interests

The authors declare that they have no conflict of interest.

References

1. McGill MR, Du K, Weemhoff JL, Jaeschke H. Critical review of resveratrol in xenobiotic-induced hepatotoxicity. *Food Chem Toxicol* 2015;86:309-18.

2. Borm PJ, Kreyling W. Toxicological hazards of inhaled nanoparticles potential implications for drug delivery. *J Nanosci Nanotechnol* 2004;4:521-31.
3. Chen Y, Xue Z, Zheng D, Xia K, Zhao Y, Liu T, et al. Sodium chloride modified silica nanoparticles as a non-viral vector with a high efficiency of DNA transfer into cells. *Curr Gene Ther* 2003;3:273-9.
4. Fisher J, Egerton TA. *Encyclopedia of Chemical Technology*. Wiley & Sons, New York 2001.
5. Kaida T, Kobayashi K, Adachi M, Suzuki F. Optical characteristics of titanium oxide interference film and the film laminated with oxides and their applications for cosmetics. *J Cosmet Sci* 2004;55:219-20.
6. Matteo C, Andrea P, Marcella M, Marco P, Chiara F, Francesca B, et al. Titanium Dioxide Nanoparticle Penetration into the Skin and Effects on HaCaT Cells. *Int J Environ Res Public Health* 2015;12:9282-97.
7. Schulz J, Hohenberg H, Pflücker F, Gärtner E, Will T, Pfeiffer S, et al. Wittern, Distribution of sunscreens on skin. *Adv Drug Deliv Rev* 2002;54:157-63.
8. Oberdörster G, Sharp Z, Atudorei V, Elder A, Gelein R, Lunts A, et al. Extrapulmonary translocation of ultrafine carbon particles following whole-body inhalation exposure of rats. *J Toxicol Environ Health A* 2002; 65:1531-43.
9. Fabian E, Landsiedel R, Ma-Hock L, Wiench K, Wohlleben W, van Ravenzwaay B. Tissue distribution and toxicity of intravenously administered titanium dioxide nanoparticles in rats. *Arch Toxicol* 2008;82:151-7.
10. Sugibayashi K, Todo H, Kimura E. Safety evaluation of titanium dioxide nanoparticles by their absorption and elimination profiles. *J Toxicol Sci* 2008;33:293-8.
11. Long TC, Tajuba J, Sama P, Saleh N, Swartz C, Parker J, et al. Nanosize titanium dioxide stimulates reactive oxygen species in brain microglia and damages neurons in vitro. *Health Perspect* 2007;115:1631-7.
12. Wang J, Li N, Zheng L, Wang S, Wang Y, Zhao X, et al. P38-Nrf-2 Signaling Pathway of Oxidative Stress in Mice Caused by Nanoparticulate TiO₂. *Biol Trace Elem Res* 2011; 140:186-97.
13. Osano E, Kishi J, Takahashi Y. Phagocytosis of titanium particles and necrosis in TNF-alpha-resistant mouse sarcoma L929 cells. *Toxicol In Vitro* 2003;17:41-7.
14. Liu HT, Ma LL, Zhao JF, Liu J, Yan JY, Ruan J, et al. Biochemical toxicity of mice caused by nano-anatase TiO₂ particles. *Biol Trace Elem Res* 2009;129:170-80.
15. Ma LL, Zhao JF, Wang J, Duan YM, Liu J, Li N, et al. The acute liver injury in mice caused by nano-anatase TiO₂. *Nanoscale Res Lett* 2009;4:1275-85.
16. Li JJ, Muralikrishnan S, Ng CT, Yung LY, Bay BH. Nanoparticle-induced pulmonary toxicity. *Exp Biol Med* 2012;235:1025-33.
17. Cui Y, Gong X, Duan Y, Li N, Hu R, Liu H, et al. Hepatocyte apoptosis and its molecular mechanisms in mice caused by titanium dioxide nanoparticles. *J Hazard Mater* 2010;183:874-80.
18. Frei B, Higdon JV. Antioxidant activity of tea polyphenols in vivo: evidence from animal studies. *J Nutr* 2003;133:3275-84.
19. Mehana EE, Meki AR, Fazili KM. Ameliorated effects of green tea extract on lead induced liver toxicity in rats, *Exp. Toxicol Pathol* 2012; 64:291-5.
20. Armanini D, De Palo CB, Mattarello MJ, Spinella P, Zaccaria M, Ermolao A, et al. Effect of licorice on reduction of body fat mass in healthy subjects. *J Endocrinol Invest* 2003;26:646-50.
21. Fenwick GR, Lutowski J, Nieman C. Glycyrrhizic acid L-composition, uses and analysis. *Food Chem* 1990;38:119-43.
22. Ma SK, Bae EH, Kim IJ, Choi KC, Kim SH, Lee J, et al. Increased renal expression of nitric oxide synthase and atrial natriuretic peptide in rats with glycyrrhizic acid-induced hypertension. *Phytother Res* 2009;23:206-11.
23. Racková L, Jancinová V, Petříková M, Drábíková K, Nosál R, Stefek M, et al. Mechanism of anti-inflammatory action of liquorice extract and glycyrrhizin. *Nat Prod Res* 2007;21:1234-41.
24. Kim SW, Jin Y, Shin JH, Kim ID, Lee HK, Park S, et al. Glycyrrhizic acid affords robust neuroprotection in the postischemic brain via anti-inflammatory effect by inhibiting HMGB1 phosphorylation and secretion. *Neurobiol Dis* 2012;46:147-56.
25. Ni B, Cao Z, Liu Y. Glycyrrhizin protects spinal cord and reduces inflammation in spinal cord ischemia-reperfusion injury. *Int J Neurosci* 2013;123:745-51.
26. Fiore C, Eisenhut M, Krausse R, Ragazzi E, Pellati D, Armanini D, et al. Antiviral effects of Glycyrrhiza species. *Phytother Res* 2008;22:141-8.
27. Smolareczyk R, Cichoń T, Matuszczak S, Mitrus I, Lesiak M, Kobusińska M, et al. The role of Glycyrrhizin, an inhibitor of HMGB1 protein, in anticancer therapy. *Arch Immunol Ther Exp* 2012;60:391-9.
28. Li XL, Zhou AG, Zhang L, Chen WJ. Antioxidant status and immune activity of Glycyrrhizin in allergic rhinitis mice. *Int J Mol Sci* 2011;12:905-16.
29. Wan XY, Luo M, Li XD, He P. Hepatoprotective and anti-hepatocarcinogenic effects of glycyrrhizin and matrine. *Chem Biol Interact* 2009;181:15-9.
30. Mabuchi A, Wake K, Marlini M, Watanabe H, Wheatley AM. Protection by glycyrrhizin against warm ischemia-reperfusion-induced cellular injury and derangement of the microcirculatory blood flow in the rat liver. *Microcirculation* 2009;16:364-76.
31. Lee CH, Park SW, Kim YS, Kang SS, Kim JA, Lee SH, et al. Protective mechanism of Glycyrrhizin on acute liver injury induced by carbon tetrachloride in mice. *Biol Pharm Bull* 2007; 30:1898-904.

176 The effect of glycyrrhizin acid on Bax and Bcl2 expression

32. Guo XL, Liang B, Wang XW, Fan FG, Jin J, Lan R, et al. Glycyrrhizic acid attenuates CC14-induced hepatocyte apoptosis in rats via a p53-mediated pathway. *World J Gastroenterol* 2013;19:3781-91.
33. Krutovskikh VA, Piccoli C, Yamasaki H. Gap junction intercellular communication propagates cell death in cancerous cells. *Oncogene* 2002;21:1989-99.
34. Soufy H, Yassein S, Ahmed AR, Khodier MH, Kutkat MA, Nasr SM, et al. Antiviral and immune stimulant activities of glycyrrhizin against duck hepatitis virus. *Afr J Tradit Complement Altern Med* 2012;9:389-95.
35. Tsai JJ, Kuo HC, Lee KF, Tsai TH. Glycyrrhizin represses total parenteral nutrition-associated acute liver injury in rats by suppressing endoplasmic reticulum stress. *Int J Mol Sci* 2013;14:12563-80.
36. Zhang R, Niu Y, Li Y, Zhao C, Song B, Li Y, et al. Acute toxicity study of the interaction between titanium dioxide nanoparticles and lead acetate in mice. *Environ. Toxicol Pharmacol* 2010;30:52-60.
37. Liang XJ, Chen C, Zhao Y, Jia L, Wang PC. Biopharmaceutics and therapeutic potential of engineered nanomaterials. *Curr. Drug Metab* 2008;9:697-709.
38. Khorsandi LS, Hashemitabar M, Orazizadeh M, Albughobeish N. Dexamethasone effects on Fas ligand expression in mouse testicular germ cells. *Pak J Biol* 2008;11:2231-6.
39. Orazizadeh M, Khorsandi LS, Hashemitabar M. Toxic effects of dexamethasone on mouse testicular germ cells. *Andrologia* 2010;42:247-53.
40. Afkhami-Ardakani M, Shirband A, Golzadeh J, Asadi-Samani M, Latifi E, Kheylapour M, et al. The effect of iron oxide nanoparticles on liver enzymes (ALT, AST and ALP), thyroid hormones (T3 and T4) and TSH in rats. *J Shahrekord Univ Med Sci* 2013;14:82-8.
41. Olmedo D, Guglielmotti MB, Cabrini RL. An experimental study of the dissemination of titanium and zirconium in the body. *J Mater Sci Mater Med* 2002;13:793-6.
42. Shukla RK, Kumar A, Pandey AK, Singh SS, Dhawan A. Titanium dioxide nanoparticles induce oxidative stress-mediated apoptosis in human HepG2 cells. *J Biomed Nanotechnol* 2011;7:100-1.
43. Li N, Duan Y, Hong M, Zheng L, Fei M, Zhao X, et al. Spleen injury and apoptotic pathway in mice caused by titanium dioxide nanoparticles. *Toxicol Lett* 2010;195:161-8.
44. Kang BPS, Urbonas A, Baddoo A, Baskin S, Malhotra A, Meggs LG. IGF-1 inhibits the mitochondrial apoptosis program in mesangial cells exposed to high glucose. *Am J Physiol Renal Physiol* 2003;285:1013-24.
45. Sohaebuddin SK, Thevenot PT, Baker D, Eaton JW, Tang L. Nanomaterial cytotoxicity is composition, size, and cell type dependent. *Part Fibre Toxicol* 2010;7:22.
46. Lemasters JJ. Necrapoptosis and the mitochondrial permeability transition: shared pathways to necrosis and apoptosis. *Am J Physiol* 1999;276:1-6.
47. Levin S, Bucci TJ, Cohen SM, Fix AS, Hardisty JF, LeGrand EK, et al. The nomenclature of cell death: recommendations of an ad hoc Committee of the Society of Toxicologic Pathologists. *Toxicol Pathol* 1999;27:484-90.
48. Gwak GY, Moon TG, Lee DH, Yoo BC. Glycyrrhizin attenuates HMGB1-induced hepatocyte apoptosis by inhibiting the p38-dependent mitochondrial pathway. *World J Gastroenterol* 2012;18:679-84.
49. Tang B, Qiao H, Meng F, Sun X. Glycyrrhizin attenuates endotoxin-induced acute liver injury after partial hepatectomy in rats. *Braz J Med Biol Res* 2007;40:1637-46.
50. Sadauskas E, Wallin H, Stoltenberg M, Vogel U, Doering P, Larsen A, et al. Kupffer cells are central in the removal of nanoparticles from the organism. *Part Fibre Toxicol* 2007;4:1-10.
51. Möller W, Hofer T, Ziesenis A, Karg E, Heyder J. Ultrafine particles cause cytoskeletal dysfunctions in macrophages. *Toxicol Appl Pharmacol* 2002;182:197-207.
52. Sun SJ, Yu WQ, Zhang YL, Jiang XQ, Zhang FQ. Effects of TiO₂ nanotube layers on RAW 264.7 macrophage behaviour and bone morphogenetic protein-2 expression. *Cell Prolif* 2013;46:685-94.
53. Duan Y, Li N, Hong M, Zheng L, Fei M, Zhao X, et al. Spleen injury and apoptotic pathway in mice caused by titanium dioxide nanoparticles. *Toxicol Lett* 2010;195:161-8.
54. Kim YA, Lee WH, Choi YH. Involvement of p21WAF1/CIP1, pRB, bax and NF-kappaB in induction of growth arrest and apoptosis by resveratrol in human lung carcinoma A549 cells. *Int J Oncol* 2010;23:1143-9.